

Original article

Radiation Dosimetry of ^{68}Ga in PET Imaging: Impact of Exposure Pathways and Age on Effective Dose and Organ-Specific Coefficients

Jemila Mussa* , Abdulwahhab Elkuwafi , Mofeda Jabr 

Department of Physics, Faculty of Science, Omar Al-Mukhtar University, Libya

Corresponding Email. jemila.mussa@omu.edu.ly

Abstract

The study investigated Positron Emission Tomography (PET), a diagnostic imaging technique employed in healthcare to evaluate physiological functions and detect abnormalities. It emphasized concerns regarding radiation dosimetry and potential risks, advocating for an evaluation of radiopharmaceuticals such as Gallium-68 (^{68}Ga) to prioritize patient safety and prevent radiation exposure. The study determined effective doses and organ-specific dose coefficients, utilizing data from the Federal Guidance Report No. 13 Database (FGR13_DB) and the International Commission on Radiological Protection (ICRP) database, for ^{68}Ga radiopharmaceutical employed in PET imaging, encompassing both internal and external exposure pathways. Younger individuals exhibited greater susceptibility to the effects of radionuclides, with internal exposure leading to significantly higher radiation doses. Consequently, incorporating age-specific coefficients is crucial when assessing the effects and risks associated with radiation exposure. The dose coefficients for ^{68}Ga exhibited variability depending on the exposure scenario. Furthermore, the organs exhibiting the highest sensitivity to radiation were determined based on the specific exposure scenario. For external exposure, the skin, breast surface, and testes were the organs most susceptible to radiation. Regarding internal exposure, the stomach wall and small intestine wall were the organs most affected by ingestion, while the esophagus, stomach wall, and small intestine wall exhibited the highest sensitivity to radiation exposure via inhalation. Concerning the effective dose, it was found that the effective dose is higher when exposure is through ingestion or the dietary route. The collected specific data of dose estimates is important for characterizing patient doses, and specific dosimetric information assists in establishing the risk and optimization of PET.

Keywords: Organ-Specific Dose Coefficients, FGR13_DB, Gallium-68 (^{68}Ga), Radiopharmaceuticals.

Introduction

Positron emission tomography (PET) is a technique that assesses physiological function by evaluating blood flow, metabolism, neurotransmitter activity, and the distribution of radiolabeled medications. It provides quantitative studies that enable the monitoring of relative changes over time as a disease process advances or in response to a specific stimulus [1]. Radionuclide small quantities of radioactive material to generate images of internal organs. Low-level radiotracers are administered orally in small doses or intravenously. Subsequently, these radiotracers bind to specific organs or tissues. Once the radioactive material enters the target organ, it breaks down by releasing a positron and annihilating with an electron in the tissues around it. This annihilation happens, and the energy of rest is released as two photons moving in opposite directions and each having an energy of 511 keV. The penetrating depth of a positron into tissue before annihilation is determined by its energy, and Certain radiation detectors can detect this radiation [2]. The advantages of PET extend beyond its diagnostic capabilities since it is so vital for guiding treatment regimens and measuring the efficacy of drugs. Positron emission tomography, like any other medical imaging procedure, has flaws and hazards. For example, ionizing radiation is utilized, making the patient radioactive for an irregular period [3]. Therefore, it is vital to undertake an evaluation of radiopharmaceuticals employed for diagnostic imaging. This research focuses on ^{68}Ga . Producing ^{68}Ga via a generator system has various benefits, including the radionuclide's easy and on-demand availability, as well as its comparatively long half-life of 67.7 minutes. These features make ^{68}Ga a flexible and frequently utilized radioisotope for a variety of PET imaging applications in clinical and research contexts [4]. This research will evaluate the radiation dose coefficients for external and internal exposure to this radionuclide, as well as the effective dose from internal exposure.

Methods

In this section, further information is extended on the assessment of the data of the selected radionuclide of the research in terms of decay, activity, integrated activity, specific activity, and average energy for this radionuclide. These criteria are critical for assessing the risks posed by radionuclides and the quality of photographs produced. Furthermore, these calculations assist in understanding the radionuclide and the potential influence that they have on health, followed by the computation of the dose coefficients for the organs for all exposure scenarios. This includes estimating dose coefficients through the FGR13_DB program and determining the effective dosage using the ICRP68_72 software while taking into account various age groups.

Decay Data

Integrated Activity

The integrated activity \tilde{A} (Bq.s) in radiation physics is defined as the total amount of radioactive substance in a sample or source. It is computed by multiplying the source's activity (A) by the duration of the activity (t):

$$\tilde{A} = At \quad (1)$$

The number of disintegrates in the source region, is calculated as the area under the curve ($A(r_s, t)$), as illustrated in Figure 1, which displays activity in the source region as a function of time after radiopharmaceutical administration. Typically, the time-integration period is set to last from the time the radiopharmaceutical is injected until infinity. Nonetheless, the integration period and the time frame during which the relevant absorbed dosage is provided (T_D) should match with the biological result under inquiry, which is [5]:

$$\tilde{A} = \int_0^{T_D} A(r_s, t) dt \quad (2)$$

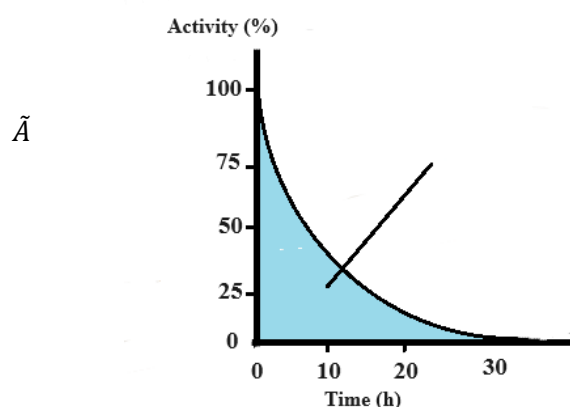


Figure 1. Radioactive decay over time[6].

Specific Activity

In nuclear medicine, a specific activity A_s (Bq/kg) is the radioactivity of a material per unit mass or mole to generate and distribute radiopharmaceuticals for therapeutic or diagnostic reasons. It is computed using the following equation:

$$A_s = \frac{\lambda N_a}{M} \quad (3)$$

where M is the radionuclide's molar mass and N_a is the Avogadro number. [8, 9].

Mean Energy \bar{E}

The average energy of beta particles emitted during radioactive decay is known as the mean energy of a beta spectrum. It is useful for understanding the proven behavior of radionuclides and their impact on human health. Equation 4 may be used to compute it[9]:

$$\bar{E} = \frac{\sum Y_i * E_i}{\sum Y_i} \quad (4)$$

where Y_i is the radiation's intensity, and E_i is its energy. The graph linking the energies in (MeV) on the x-axis to the intensity on the y-axis may also be used to calculate the beta spectrum's endpoint energy and mean energy. After obtaining the decay data for the radionuclide ^{68}Ga .

Submersion Dose Coefficient

The submersion dose coefficient h_T (Sv/ Bq.s m⁻³) is a metric used to assess radiation exposure when a person is immersed in a radioactive environment, such as radioactive air or water. The energy of ionizing radiation to materials in a limited volume is measured to calculate the absorbed dose. The absorbed dose (D) may be calculated using the mean energy (\bar{E}_T) of ionizing radiations supplied to a certain mass (m) inside a volume (V). It follows the radiation protection scheme outlined by the ICRP [10]. The coefficients are calculated based on the weighting factors stated in ICRP1991, with an air density of 1.2 kg m⁻³. Where h_T is the dose equivalent per unit time-integrated exposure to a radionuclide, and h_E is the effective dose equivalent per unit time-integrated exposure to a radionuclide as shown in following equation (Saito *et al.*, 2012)

$$h_E = \sum_T w_T h_T \quad (5)$$

Ground Plane Dose Coefficient (Sv / Bq.s m⁻²)

The horizontal reference surface is utilized for dose estimates and radiation measurements, and it serves as a standard for measuring radiation doses and exposure. It examines scenario geometry, shielding effects, and distance from the radiation source. Radiation transport codes and mathematical models may be employed in specific calculations. Radionuclides can persist on and in the ground for long years, possibly exposing the population for radiation [11].

Soil Volume Dose Coefficient (Sv/ Bq.s m⁻³)

This coefficient is used to assess radiation exposure from contaminated soil or to assess the release of radioactive contaminants. Organ dose rate coefficients for uniformly distributed volume sources with thicknesses of 1, 5, and 15 cm, as well as an essentially infinite source, were calculated by combining organ dose rate coefficients for isotropic plane sources at six depths. The dosage rate coefficient for a volumetric source with uniform activity concentration may be calculated using the equation:

$$\hat{h}_{T,L}(\epsilon) = \frac{1}{\mu} \int_0^{\mu L} \hat{h}_{T,P}(\epsilon, \tau) d\tau \quad (6)$$

Where $\hat{h}_{T,P}(\epsilon, \tau)$ indicates the dose rate coefficient for tissue T , planar source P at energy ϵ and depth τ (mean free path), at energy ϵ , μ is the soil's linear attenuation coefficient [12].

Internal Exposure Dose Coefficient

Radionuclides enter the body by inhalation, ingestion, or injection, exposing it to ionizing radiation. This exposure ceases when the radionuclide is removed from the body, whether naturally or by medical intervention. Dosimetric models will be used to study radionuclides' time-dependent activities once they enter the body. The models will be done for six ages: infant, 1 year, 5 years, 10 years, 15 years, and adult. Dosimetric models involve two types of body areas: source regions and target regions. Source areas are the locations of radioactivity, whereas target regions are organs and tissues that can calculate radiation dose. Aerosol inhalation coefficients are determined using values like 3 g/cm², 1.5 form factor, 2.5 geometric standard deviation, and an activity median aerodynamic diameter (AMAD) of 1 μ m [13].

Organ-Specific Dose Coefficients

Organ-specific dose coefficients are used to quantify the absorbed dose of a known radiation exposure in an organ or tissue. They are commonly stated as the ratio of the absorbed dosage in the organ or tissue to the air kerma at a reference site in the body [14]. Organ-specific dose coefficients are values used to quantify the quantity of radiation that specific organs or body parts will be exposed to during the diagnostic imaging process. These coefficients are calculated using complex computations, reference computation alphantoms provided by organizations like the ICRP, and radiation transport methods like Monte Carlo N-Particle (MCNP). Dose coefficients are essential for radiation protection and optimizing medical therapies by identifying possible health issues, which contributes to informed decisions to decrease radiation exposure while achieving the required diagnostic or therapeutic results [15,12].

Effective Dose (E_D)

In radiation protection, the effective dose is a statistic for calculating the potential harm caused by ionizing radiation exposure. It takes into account the kind and energy of radiation, as well as the susceptibility of different organs and tissues to radiation damage. The effective dose is measured in (Sv) or (mSv). The effective dosage is obtained using the effective dose coefficients, also known as tissue weighting factors, and derived by the following equation:

$$E_D = \sum_T w_T \cdot H_T \quad (7)$$

where E_D denotes the effective dosage and w_T represents the tissue weighting factor. The effective dosage coefficients are debated and suggested by the ICRP [16, 17].

Results and Discussion

The results of the integrated activity \tilde{A} of the radionuclide was presented in Figure 2. The integrated activity is demonstrating the total quantity of radioactive material in a sample or source over an interval of time. The figure depicts how the integrated activity increases over time until it achieves a constant value, suggesting that the radioactive decay process has stabilized. After 800 minutes, the integrated activity reached its peak value of 5.86×10^3 Bq/s. The specific activity A_s of radioisotope ⁶⁸Ga was 1.5×10^{21} Bq/kg.

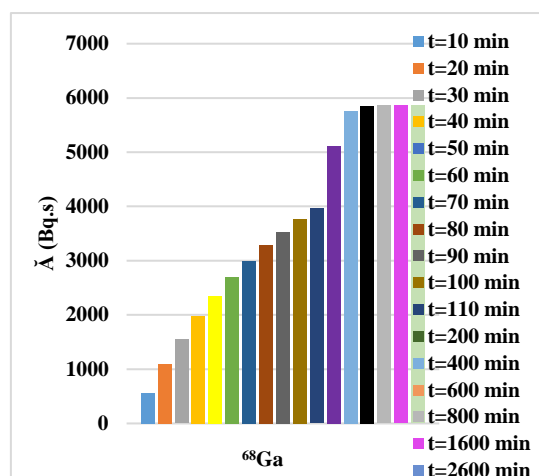


Figure 2. The variation of radioactivity of a ^{68}Ga sample over time.

Average Energy \bar{E}

Figure 3 illustrates the beta particle energy and intensity spectrum of ^{68}Ga . The spectrum exhibits an endpoint energy of 1.9 MeV and an average energy of 0.830 MeV. These data are fundamental for precise calculations in radiation dosimetry, medical imaging, and radiation safety applications. On the other hand, Table 1 contains comprehensive decay statistics and displays the type of radiation, radiation intensity, total energy, and average energy for the radioisotope ^{68}Ga . The data allows the decay characteristics and behavior of radionuclides, offering vital insights into their radioactive decay kinetics and emission rates.

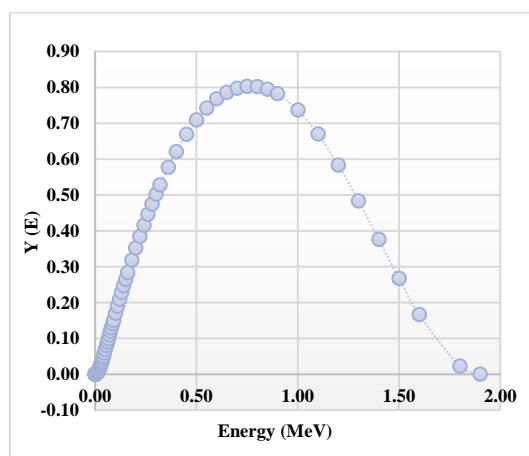


Figure 3. Beta particle energy distribution of ^{68}Ga .

Table 1. Radiation characteristics of ^{68}Ga .

| Radiation | Frequency(/nt) | average (MeV / nt) | Mean Energy (MeV) |
|----------------------|-----------------------|-----------------------|-----------------------|
| Gamma rays | 3.59×10^{-2} | 3.96×10^{-2} | 1.13×10^{-2} |
| X-rays | 5.68×10^{-1} | 4.07×10^{-4} | 7.15×10^{-4} |
| Inhalation quanta | 1.77×10^{-2} | 9.08×10^{-1} | 5.11×10^{-1} |
| Beta+ | 8.89×10^{-1} | 7.37×10^{-1} | 8.29×10^{-1} |
| IC electrons | 9.32×10^{-6} | 9.79×10^{-6} | 1.05×10^{-2} |
| Auger electrons | 4.10×10^{-1} | 5.49×10^{-4} | 1.33×10^{-3} |
| Total emitted energy | | 1.68 | |

Submersion Dose Coefficients (Sv/Bq.s m^{-3})

Figure 4 depicts the examination of submersion dose coefficients for ^{68}Ga across several anatomical areas, yielding significant results for understanding the varied vulnerability of these regions to submersion doses. Among the organs considered, the Skin, B_surface, and Breasts exhibited the highest submersion dose coefficients, with values of 1.01×10^{-13} , 7.84×10^{-14} , and 5.11×10^{-14} , respectively. In contrast, the ovaries displayed the lowest submersion dose coefficient. These data highlight the diverse sensitivity of anatomical locations to ^{68}Ga submersion doses, with notable heterogeneity in organ response to submersion irradiation.

Ground Plane Dose Coefficients (Sv/Bq.s m⁻²)

A notable level of heterogeneity is observed in the ground plane dose coefficients for ⁶⁸Ga, as evidenced in Figure 5. The skin demonstrated the highest dose coefficient (1.00×10^{-14} Sv/Bq.s m⁻²), followed by the B_surface (1.37×10^{-15} Sv/Bq.s m⁻²) and the Testes (9.89×10^{-16} Sv/Bq.s m⁻²). In contrast, the esophagus exhibited the lowest dose coefficient, with a value of 7.66×10^{-16} Sv/Bq.s m⁻².

Soil Volume Dose Coefficients (Sv/Bq.s m⁻³)

A discernible pattern emerges regarding the soil volume dose coefficients and their corresponding impacts on different organs, as illustrated in Figure 4. An interesting finding is that the ranking order of the soil volume dose coefficient is similar to that of the submersion dose coefficient across different organs, with the exception that the order of the highest values of the soil volume dose coefficient for the organs differed slightly from the order of the submersion dose coefficient. The soil volume dose coefficients for B_surface, skin, and breasts were 4.80×10^{-17} , 4.13×10^{-17} , and 3.26×10^{-17} Sv/Bq.s m⁻³, respectively, while the submersion dose coefficients were also greatest for B_surface, Breasts, and Skin. The soil volume dose coefficient was likewise less than the submersion dose coefficient for the same organs. The pancreas has the lowest coefficient at 2.32×10^{-17} Sv/Bq.s m⁻³.

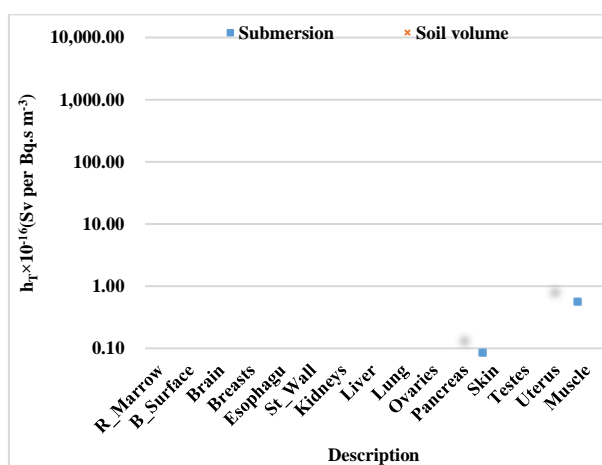


Figure 4. Submersion and Soil Volume Dose Coefficients of ⁶⁸Ga.

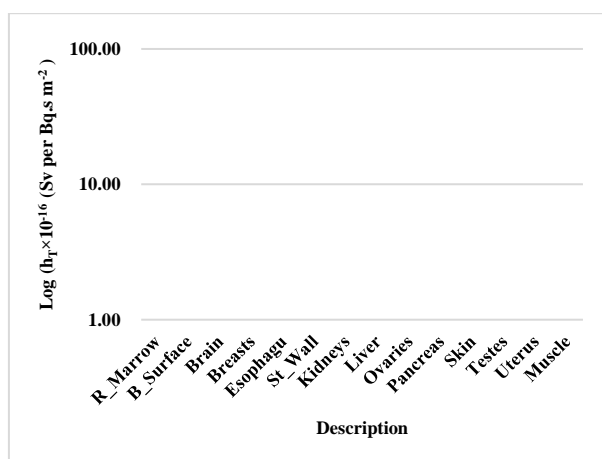


Figure 5. Ground plane dose coefficients of ⁶⁸Ga.

Internal Exposure Dose Coefficient

The ingestion dose coefficients for radionuclide ⁶⁸Ga, provide valuable insights into the effects that occur for radiation exposure to various organs across different developmental stages. As illustrated in Figure 6, the study examined the age-dependent variations in ingestion dose coefficients for infants, 1 y, 5 y, 10 y, 15 y, and adults. After analyzing data, St_wall had the greatest ingestion dose coefficient with values of 7.10×10^{-9} , 3.92×10^{-9} , 1.92×10^{-9} , 1.10×10^{-9} , 7.61×10^{-10} , and 5.97×10^{-10} Sv/Bq for infantes, 1 y, 5 y, 10 y, 15 y, and adults. The SI_wall exhibited the second highest ingestion dose coefficients, decreasing from 4.71×10^{-9} Sv / Bq in infants to 4.18×10^{-10} Sv/Bq in adults. The ingestion dose coefficients exhibit an inversely proportional relationship with age, with the brain having the lowest values across all ages. Inhalation dose coefficients for type F, M, and S particulates were evaluated for various organs and age groups (infants, 1 y, 5 y, 10 y, 15 y, and adults), as depicted in Figure 7. The analysis demonstrates that the ET_Region, St_wall, and SI_wall consistently exhibit the highest sensitivity to inhaled radiation across

all age groups, indicating a significant vulnerability of these organs to internal radioactive particle deposition. Inhalation dose coefficients for type F particles in the ET_Region demonstrate a significant age-dependent decrease, with infants exhibiting the highest value $3.64 \times 10^{-9} \text{Sv/Bq}$, followed by a gradual decline to $4.15 \times 10^{-10} \text{Sv/Bq}$ in adults. This pattern is observed for type F, M, and S particles, with the testes consistently exhibiting the lowest dose coefficients, suggesting a lower susceptibility to inhaled radiation. The ET_Region demonstrated the highest sensitivity to inhaled type M particles, with infants exhibiting the highest dose coefficients with value of $4.85 \times 10^{-9} \text{Sv/Bq}$. This sensitivity decreased significantly with age to the values 4.85×10^{-9} , 3.80×10^{-9} , 1.79×10^{-9} , 1.11×10^{-9} , 6.32×10^{-10} , and $5.39 \times 10^{-10} \text{Sv/Bq}$, for the mentioned above ages, respectively. St_wall and Lung are likewise very sensitive to these particles, with different inhalation dosage factors according on age. ET_Region has the highest inhalation dose coefficient for type S particles, with values of 4.85×10^{-9} , 3.80×10^{-9} , 1.79×10^{-9} , 1.11×10^{-9} , 6.32×10^{-10} , and $5.39 \times 10^{-10} \text{Sv/Bq}$ for infants, 1 y, 5 y, 10 y, 15 y, and adults, respectively. The ranking of organs based on dose coefficient sensitivity for type S particles follows a similar trend as that observed for types F and M, with the testes consistently showing the lowest susceptibility.

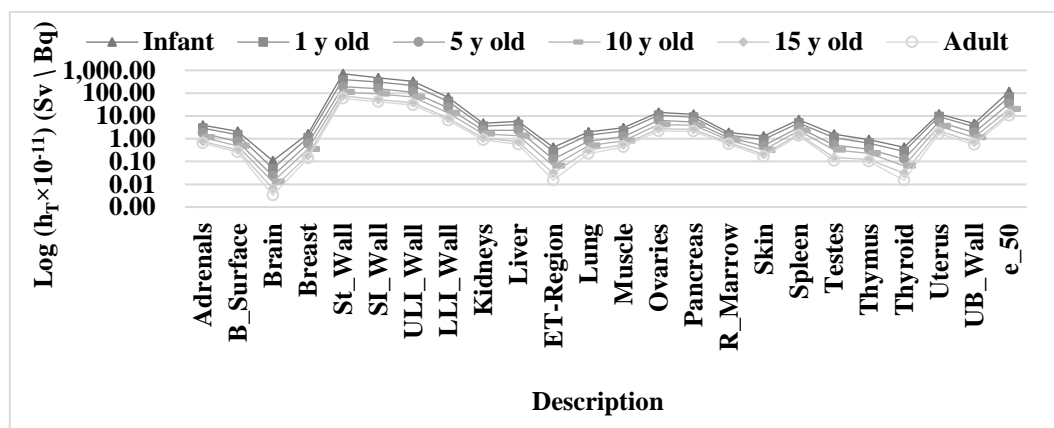


Figure 6. Differences in organ radiosensitivity to ingested ^{68}Ga across different age groups.

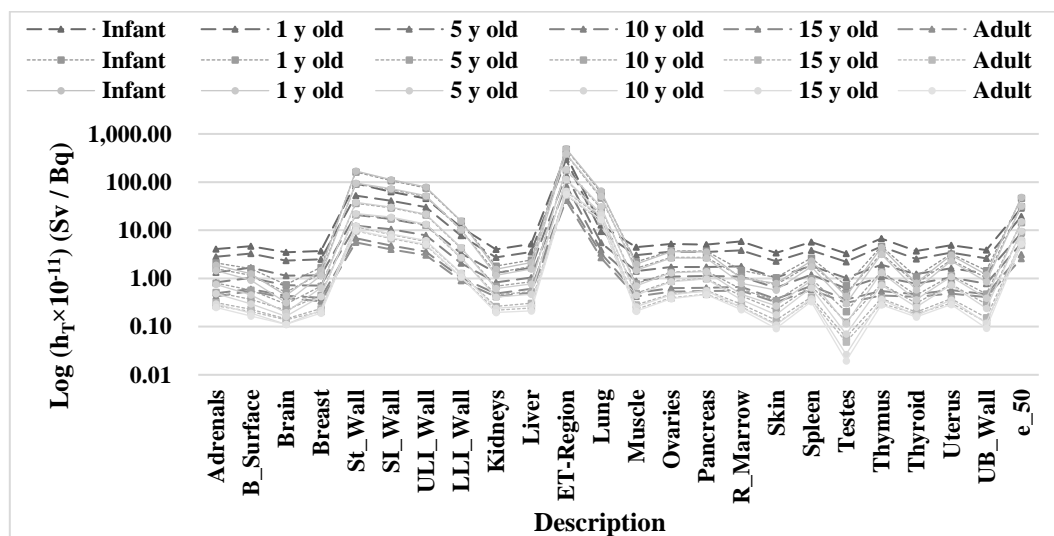


Figure 7. Differences in inhalation dose coefficients among different ages and organs from particulate type F, M, and S for ^{68}Ga .

Effective Dose (Sv)

A comparison of effective doses from various exposure pathways reveals that ingestion poses the greatest radiological risk to the general population exposed to 1-micron aerosols of the radionuclide. This is evident from the higher effective dose values associated with ingestion compared to other exposure routes. This comparative analysis of effective doses highlights the varying impact of ^{68}Ga radionuclide exposure on different segments of the general population.

Table 2. Effective doses from inhalation and ingestion of 68Ga in different age groups. Intake routes Age.

| Intake routs | | Age | | | | | |
|--------------|---------|-----------|-----------|-----------|-----------|-----------|-----------|
| | | Infant | 1 y | 5 y | 10 y | 15 y | Adult |
| Inhalation | Type: F | 2.9×10-10 | 1.9×10-10 | 8.8×10-11 | 5.4×10-11 | 3.1×10-11 | 2.6×10-11 |
| | Type: M | 4.6×10-10 | 3.1×10-10 | 1.4×10-10 | 9.2×10-11 | 5.9×10-11 | 4.9×10-11 |
| Ingestion | | 1.2×10-9 | 6.7×10-10 | 3.4×10-10 | 2.0×10-10 | 1.3×10-10 | 1.0×10-10 |

Conclusion

The study findings indicate that internal exposure to radionuclides poses a significantly greater radiological risk than external exposure. This is primarily due to the continuous internal radiation source, which delivers a sustained dose to surrounding tissues. Furthermore, the close proximity of internally deposited radionuclides to cellular structures significantly enhances the potential for biological damage. The organs most sensitive to radiation were determined based on the exposure scenario. For external exposure, the Skin, B_surface, and Testes are the most affected organs due to their proximity to the external radiation source, resulting in the highest direct radiation dose. Also due to the lack of adequate protection. Regarding internal exposure, St_wall and SI_wall exhibited the highest dose coefficients following ingestion. This sensitivity is attributed to several factors, including the direct exposure of the digestive tract lining to ingested radionuclides, rendering it vulnerable to radiation-induced damage. A significant portion of the radionuclide is absorbed through the small intestinal wall, increasing the likelihood of interactions with sensitive cells. The ET_Region, St_wall, and SI_wall are among the organs most sensitive to radiation exposure following inhalation. This sensitivity arises from direct exposure to the respiratory system, where the bronchi and lungs are initially exposed to inhaled radioactive particles. Furthermore, if inhaled particles or contaminated phlegm are subsequently swallowed, the stomach and small intestine are directly exposed to the radionuclide. The evaluated effects of the radionuclide were found to be more pronounced in younger age groups, emphasizing the importance of considering age-specific dose coefficients when assessing radiation risks. The study also found that inhaled radiation for slow-absorbing particles (Type S) has higher dose coefficients compared to medium-absorbing particles (Type M) and fast-absorbing particles (Type F). With regard to the effective dose, it was found that higher effective doses were observed when exposure occurred through ingestion or the dietary route. Effective doses were also found to be greater in younger age groups. While this study provides valuable insights into the dosimetric effects of these substances, further research is needed to fully comprehend the complexities of radiation exposure in diagnostic imaging. A systematic evaluation of all radionuclides used in clinical practice is essential to identify potential knowledge gaps and inform future radiation protection strategies.

Acknowledgments

The authors thank the Physics Department for supporting and approving this research.

Conflicts of Interest

There are no financial, personal, or professional conflicts of interest to declare.

References

- Berger A. Positron emission tomography. *Br Med J*. 2003;326(7404):1449. <https://doi.org/10.1136/bmj.326.7404.1449>.
- Wagner HN Jr. A brief history of positron emission tomography (PET). *Semin Nucl Med*. 1998;28(3):213-220. [https://doi.org/10.1016/S0001-2998\(98\)80027-5](https://doi.org/10.1016/S0001-2998(98)80027-5).
- Kasban H, El-Bendary MAM, Salama DH. A comparative study of medical imaging techniques. *Int J Inf Sci Intell Syst*. 2015;4(1):37-58.
- Velikyan I. 68Ga-based radiopharmaceuticals: production and application relationship. *Molecules*. 2015;20(7):12913-12943. <https://doi.org/10.3390/molecules200712913>.
- Lerch H, Jigalin A. Nuclear medicine: medical technology research. *Nucl Med*. 2005;44(6):267-271. <https://doi.org/10.1055/s-0038-1625324>.
- Tandon P, Prakash D, Kheruka SC, Bhat NN. Nuclear medicine internal dose assessment. In: *Radiopharmaceuticals and Translational Medicine*. Singapore: Springer Nature; 2022:281-297. https://doi.org/10.1007/978-981-19-4518-2_19.
- De Goeij JJM, Bonardi ML. How do we define the concepts specific activity, radioactive concentration, carrier, carrier-free and no-carrier-added? *J Radioanal Nucl Chem*. 2005;263(1):13-18. <https://doi.org/10.1007/s10967-005-0004-6>.
- Lapi SE, Welch MJ. A historical perspective on the specific activity of radiopharmaceuticals: what have we learned in the 35 years of the ISRC? *Nucl Med Biol*. 2012;39(5):601-608.
- Eckerman KF. Radiological Toolbox User's Manual [Technical Report OSTI 885634]. Oak Ridge, TN: U.S. Department of Energy; 2004. <https://doi.org/10.2172/885634>.
- Bellamy MB, Veinot KG, Hiller MM, et al. Effective dose rate coefficients for immersions in radioactive air and water. *Radiat Prot Dosimetry*. 2017;174(2):275-286. <https://doi.org/10.1093/rpd/ncw103>.

11. Saito K, Ishigure N, Petoussi-Hens N, Schlattl H. Effective dose conversion coefficients for radionuclides exponentially distributed in the ground. Radiat Environ Biophys. 2012;51(4):411-423. <https://doi.org/10.1007/s00411-012-0432-y>.
12. Veinot KG, Eckerman KF, Bellamy MB, et al. Effective dose rate coefficients for exposure to contaminated soil. Radiat Environ Biophys. 2017;56(3):255-267. <https://doi.org/10.1007/s00411-017-0692-7>.
13. Haaker RF, Bixler NE, Marrow RB. FGR 13 Dose Conversion Factor Files Breast. 2018.
14. Taulbee TD, McCartney KA, Traub R, Smith MH, Neton JW. Implementation of ICRP 116 dose conversion coefficients for reconstructing organ dose in a radiation compensation program. Radiat Prot Dosimetry. 2017;173(1):131-137. <https://doi.org/10.1093/rpd/ncw305>.
15. Jansen JTM, Shrimpton PC, Edyvean S. CT scanner-specific organ dose coefficients generated by Monte Carlo calculation for the ICRP adult male and female reference computational phantoms. Phys Med Biol. 2022;67(22):225015. <https://doi.org/10.1088/1361-6560/ac9e3d>.
16. Harrison JD, Balonov M, Bochud F, et al. ICRP Publication 147: use of dose quantities in radiological protection. Ann ICRP. 2021;50(1):9-82. <https://doi.org/10.1177/0146645320911864>.
17. McCollough CH, Schueler BA. Educational treatise: calculation of effective dose. Med Phys. 2000;27(5):828-837.

المستخلص

تناولت الدراسة التصوير المقطعي بالإصدار البوزيتروني وهو تقنية تصوير تشخيصي تُستخدم في مجال الرعاية الصحية لتقييم الوظائف الفسيولوجية والكشف عن التشوهات. وشهدت الدراسة على المخاوف المتعلقة بقياس جرعات الإشعاع والمخاطر المحتملة، داعيةً إلى تقييم المستحضرات الصيدلانية المشعة مثل الغاليوم-68 (^{68}Ga) لإعطاء الأولوية لسلامة المرضى ومنع التعرض للإشعاع. وحددت الدراسة الجرعات الفعالة ومعاملات الجرعة الخاصة بكل عضو، باستخدام بيانات من قاعدة بيانات تقرير التوجيه الفيدرالي رقم 13 (FGR13_DB) وقاعدة بيانات اللجنة الدولية للحماية من الإشعاع، للمستحضرات الصيدلانية المشعة ^{68}Ga المستخدمة في التصوير المقطعي بالإصدار البوزيتروني، شاملةً مسارات التعرض الداخلي والخارجي. أظهر الأفراد الأصغر سنًا قابلية أكبر لتأثيرات النويدات المشعة، حيث يؤدي التعرض الداخلي إلى جرعات إشعاعية أعلى بكثير. وبالتالي، يُعد دمج المعاملات الخاصة بالعمر أمرًا بالغ الأهمية عند تقييم الآثار والمخاطر المرتبطة بالتعرض للإشعاع. وقد أظهرت معاملات الجرعة للغاليوم-68 تباينًا تبعًا لسيناريو التعرض. علاوة على ذلك، تم تحديد الأعضاء الأكثر حساسية للإشعاع بناءً على سيناريو التعرض المحدد. بالنسبة للتعرض الخارجي، كان الجلد وسطح الثدي والخصيتين الأعضاء الأكثر عرضة للإشعاع. أما بالنسبة للتعرض الداخلي، فكان جدار المعدة وجدار الأمعاء الدقيقة الأعضاء الأكثر تأثرًا بالابتلاع، بينما أظهر المريء وجدار المعدة وجدار الأمعاء الدقيقة أعلى حساسية للتعرض للإشعاع عن طريق الاستنشاق. وفيما يتعلق بالجرعة الفعالة، وُجد أن الجرعة الفعالة تكون أعلى عند التعرض عن طريق الابتلاع أو عن طريق الغذاء. تُعد البيانات المحددة للمجموعة لتقديرات الجرعة مهمة لتوصيف جرعات المرضى، كما يساعد تكوين قياس الجرعات المحدد في تحديد مخاطر التصوير المقطعي بالإصدار البوزيتروني وتحسينه.